Journal of
Synchrotron Radiation

ISSN 0909-0495

Received 29 September 2009
Accepted 26 November 2009

Concept of a spectrometer for resonant inelastic X-ray scattering with parallel detection in incoming and outgoing photon energies

V. N. Strocov

Swiss Light Source, Paul Scherrer Institute, 5232 Villigen-PSI, Switzerland.
E-mail: vladimir.strocov@psi.ch

A spectrometer for resonant inelastic X-ray scattering (RIXS) is proposed where imaging and dispersion actions in two orthogonal planes are combined to deliver a full two-dimensional map of RIXS intensity in one shot with parallel detection at incoming $h\nu_{in}$ and outgoing $h\nu_{out}$ photon energies. Preliminary ray-tracing simulations with a typical undulator beamline demonstrate a resolving power well above 11000 with both $h\nu_{in}$ and $h\nu_{out}$ near 930 eV, with a vast potential for improvement. Combining this instrument – nicknamed $h\nu^2$ spectrometer – with an X-ray free-electron laser source simplifies its technical implementation and enables efficient time-resolved RIXS experiments.

Keywords: resonant inelastic X-ray scattering; X-ray optics; X-ray spectrometers; free-electron lasers.

1. Introduction

High-resolution resonant inelastic X-ray scattering (RIXS) is a synchrotron radiation based photon-in/photon-out experimental technique that provides information about charge-neutral low-energy excitations in correlated electron systems (*e.g.* crystal field, charge transfer or spin excitations) in solids, liquids and gases (Kotani & Shin, 2001).

The richness of the physical information available from RIXS depends directly on the resolution and detection efficiency of RIXS instrumentation (see Nordgren *et al.*, 1989; Hague *et al.*, 2005; Tokushima *et al.*, 2006; Ghiringhelli *et al.*, 2006; Agåker *et al.*, 2009). Soft X-ray RIXS spectrometers of the last generation (Ghiringhelli *et al.*, 2006) based on variable-line-spacing (VLS) gratings and high-resolution CCD detectors allow routine operation with a resolving power $E/\Delta E$ better than 10000 at 1 keV photon energy, which takes the RIXS experiment from the energy scale of charge-transfer and crystal-field excitations to that of orbital and magnetic excitations (Schlappa *et al.*, 2009). A position-sensitive CCD detector allows parallel detection at outgoing photon energies $h\nu_{out}$. Modern beamlines, delivering a spot size on the sample in the few micrometres range, enable slitless operation of the RIXS spectrometers, dramatically increasing their detection efficiency. An interesting concept to further increase the detection efficiency is the use of an active grating monochromator/active grating spectrometer (Fung *et al.*, 2004) which promises a gain of two orders of magnitude. Another non-conventional concept (Hatsui *et al.*, 2005) uses a transmission grating and a Wolter mirror as a pre-focusing system to dramatically increase the spectrometer acceptance angle.

The full set of RIXS data is a two-dimensional map of X-ray scattered intensity $I(h\nu_{in}, h\nu_{out})$ depending on the incoming $h\nu_{in}$ and outgoing $h\nu_{out}$ photon energies. Presently, one acquires $I(h\nu_{in}, h\nu_{out})$ in a sequential fashion by measuring one-dimensional $I(h\nu_{out})$ spectra over a series of separate $h\nu_{in}$ selected by the beamline monochromator. Here, a concept is presented for the RIXS spectrometer to enable acquisition of the whole $I(h\nu_{in}, h\nu_{out})$ map in one shot with parallel detection at $h\nu_{in}$ and $h\nu_{out}$.

2. Concept

The optical scheme of such a RIXS spectrometer – nicknamed $h\nu^2$ for simultaneous detection at $h\nu_{in}$ and $h\nu_{out}$ – is shown in Fig. 1. The monochromator produces in its (stigmatic) focal plane a line image of light with vertical dispersion in energy $h\nu_{in}$. A refocusing Kirkpatrick–Baez optics consisting of vertically and horizontally refocusing (plane-elliptical) mirrors, V-RM and H-RM, respectively, brings this image into a line focus on the sample. Extreme vertical demagnification of the refocusing stage is necessary to squeeze the vertical extension of the image, important for inhomogeneous samples, and extreme horizontal demagnification to deliver small source size and thus high energy resolution for the spectrometer operating slitless. The light scattered from the sample is intercepted by a vertically focusing (plane-elliptical) mirror V-FM of the spectrometer stage. It operates in the vertical (imaging) plane to bring the scattered light image into a magnified image on the two-dimensional position-sensitive detector (PSD) with vertical dispersion in $h\nu_{in}$. A (spherical) VLS grating operates in the horizontal (dispersive) plane to

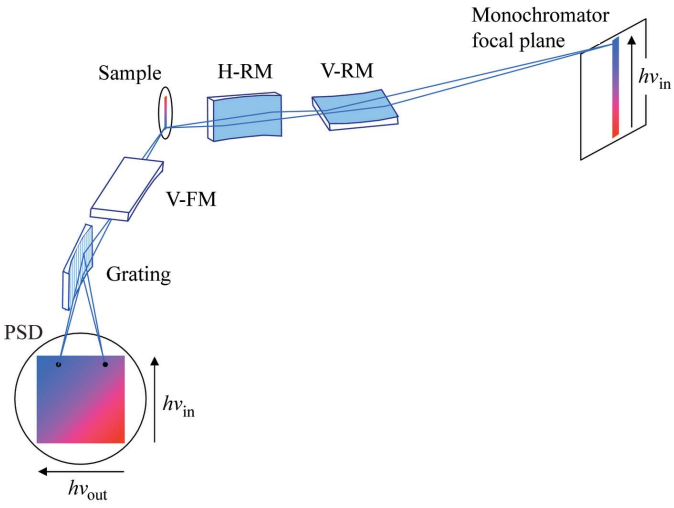

Figure 1
Operational principle of the $h\nu^2$ spectrometer. The image formed on the PSD is the full two-dimensional image of RIXS intensity $I(h\nu_{in}, h\nu_{out})$ acquired with parallel detection in $h\nu_{in}$ and $h\nu_{out}$.

disperse the scattered light in $h\nu_{out}$ and focus it onto the PSD with horizontal dispersion in $h\nu_{out}$. In this way a full two-dimensional image of RIXS intensity $I(h\nu_{in}, h\nu_{out})$ is formed on the PSD in one shot with parallel detection in $h\nu_{in}$ and $h\nu_{out}$.

The $h\nu^2$ spectrometer has the following distinctive properties:

(i) If one inserts a slit into the monochromator focal plane to select one single $h\nu_{in}$, the $h\nu^2$ spectrometer becomes fully equivalent to a standard RIXS instrument with VLS gratings (Ghiringhelli *et al.*, 2006) where the dispersive plane is horizontal and the V-FM acts to focus the beam on the CCD in the non-dispersive vertical plane, increasing the spectrometer acceptance by a factor of about three compared with the single-grating design (Hague *et al.*, 2005). Therefore, the $h\nu^2$ concept adds simultaneous detection in $h\nu_{in}$ as a 'free lunch' without compromising the detection efficiency in $h\nu_{out}$ compared with standard RIXS spectrometers. There is no compromise on resolution in $h\nu_{in}$ either, provided the horizontal demagnification is sufficient.

(ii) The $h\nu^2$ spectrometer inherently includes an option for XAS data acquisition in the total fluorescence yield in one shot of parallel detection in $h\nu_{in}$. This measurement mode is realised simply by setting the grating to the zero diffraction order. The vertical line formed in this case on the PSD is the XAS spectrum as a function of $h\nu_{in}$. Note that aberrations from the grating affect in this case only the horizontal image profile and, by integration in the horizontal direction, have no influence on the XAS spectrum. In this connection one should mention energy-dispersive XAS [see a review by Pascarelli *et al.* (2006)] which is an efficient technique for one-shot XAS data acquisition although limited by the hard X-ray energy range. XAS experiments in the soft X-ray range with single shots of a pulsed X-ray free-electron laser (XFEL) source have recently been demonstrated at FLASH by Bernstein *et al.* (2009), who used the transmission of X-rays through a thin-film sample installed in the monochromator focal plane and a PSD behind based on a fluorescent YAG crystal.

(iii) The additional detection channel can be utilized as a means to dramatically increase the detection efficiency without compromising the resolution in $h\nu_{out}$. Such a transmission mode of the $h\nu^2$ spectrometer can be achieved, in the case of normal X-ray emission characterized by $h\nu_{in}$ independent spectral structures, by integration of the PSD image along the $h\nu_{in}$ direction. In the case of RIXS, when $h\nu_{in}$ independent over certain interval are energy losses as a function of $(h\nu_{out} - h\nu_{in})$, the integration should be performed along the $h\nu_{in} = h\nu_{out}$ line with post-processing of the image. The corresponding detection efficiency increase compared with the conventional spectrometers is defined by the ratio of the intercepted $h\nu_{in}$ bandwidths, *i.e.* of the order of 5 eV compared with 100 meV, making a factor of 50.

(iv) The response of the $h\nu^2$ spectrometer as a function of $h\nu_{in}$ critically depends on the homogeneity of the sample along the line focus. However, the vertical refocusing can reduce its extension below 100 µm within an $h\nu_{in}$ bandwidth of a few eV (see the ray-tracing analysis below) which is acceptable for most of the samples. The sample homogeneity is not an issue for studies on liquids and gases.

(v) Crucial for achieving high resolution in $h\nu_{out}$ is a small horizontal spot size at the sample. With standard third-generation synchrotron sources, this requires extreme (nevertheless feasible) demagnification in the refocusing stage. Highly advantageous in this respect is further reduction of the synchrotron radiation emittance achievable with new (SOLEIL, DIAMOND) and future (PETRA III, NSLS-II) sources, ultimately XFELs.

(vi) An important aspect of the $h\nu^2$ concept compared with the usual sequential data acquisition is that the full RIXS snapshot $I(h\nu_{in}, h\nu_{out})$ of the electronic structure is acquired in the same instant of time. This is a crucial advantage for studies of time evolution processes, including the kinetics of chemical reactions.

(vii) The total optical length of the spectrometer stage has to be constant under variation of photon energy in order to stay focused in $h\nu_{in}$. Maintaining high resolution in $h\nu_{out}$ requires then two degrees of freedom of the optical system to cancel both the defocus and coma aberrations (Strocov *et al.*, 2008). They can be delivered by (coordinated) variation of the grating pitch angle and the grating translation.

Although the $h\nu^2$ concept promises an adequate performance already with common third-generation synchrotron sources (see below), its full potential unfolds with XFEL sources. Their inherently pulsed operation ideally combines with the ability of the $h\nu^2$ spectrometer to produce full $I(h\nu_{in}, h\nu_{out})$ snapshots in the same instant of time, allowing efficient time-resolved measurements (Patterson *et al.*, 2009). Furthermore, the dramatic increase of the intercepted $h\nu_{in}$ bandwidth radically alleviates the problem of low average intensity of the XFEL radiation. On the technical side, an important advantage of XFELs is a round spot profile. The much smaller horizontal source size compared with the synchrotron sources allows further reduction of the horizontal

spot size on the sample and thus an increase of resolution in $h\nu_{out}$. Furthermore, the small angular divergence of XFEL radiation helps reduce the size of the optical elements.

3. Ray-tracing simulations

The expected performance of the $h\nu^2$ spectrometer operating at a typical undulator beamline of a third-generation synchrotron source was estimated using preliminary ray-tracing simulations. No attempt was made to optimize exact parameters of the optical scheme. The simulations were performed using the code *PHASE* (Bahrdt *et al.*, 1995). In order to reduce errors of the polynomial approximation of the ellipsoidal shape (Peatman, 1997) in this code, the ray tracing was restricted around the central ray within an angular divergence of 0.01 mrad for the refocusing stage and 0.1 mrad for the spectrometer stage in the vertical (imaging) plane. Simulations in its horizontal (dispersive) plane used the code *TraceVLS* (Strocov *et al.*, 2008) without such divergence restrictions. The refocusing and spectrometer stages each had a length of 5500 mm. For all optical elements, including the grating, the light incidence angle was 88° and the slope errors were taken as 0.5 µrad r.m.s., which is a conservative state-of-the-art value for the (bendable) plane and spherical optics. The energy was chosen as 930 eV (near the $2p_{3/2}$ core level of Cu).

The *monochromator* adopts the classical collimated-light plane-grating monochromator scheme (Follath & Senf, 1997) with stigmatic focus. The source parameters (FWHM spot size $s_V \times s_H$ = 33 µm × 252 µm and angular divergence $s_V \times s_H$ = 33 µrad × 111 µrad) and positions of the optical elements (collimating mirror at 20000 mm from the source and slit at 10000 mm from the focusing mirror) are chosen close to those of the ADRESS beamline of the Swiss Light Source (Strocov *et al.*, 2010). In order to increase the horizontal demagnification, the collimating mirror is chosen to be cylindrical, with horizontal focusing performed by a focusing mirror of toroidal shape. With a grating of 1400 lines mm^{-1} and C_{ff} = 2.75, the monochromator delivers $E/\Delta E \simeq 15000$. The image in its focal plane formed by five monochromatic rays separated by 1 eV is shown in Fig. 2(*a*).

The *refocusing stage* has a total length of 5500 mm. The V-RM is installed at 500 mm from the sample and the H-RM at 200 mm, delivering extreme horizontal demagnification of the spot (combining the two Kirkpatrick–Baez mirrors in one ellipsoidal mirror results in a 'smiley' distortion of the image on the sample). With the light incident on the sample at a grazing angle of 30° and scattering angle 90°, the image seen by the spectrometer is shown in Fig. 2(*b*). Its vertical extension is less than 100 µm. Note the certain distortion of the vertical scale owing to the spatial extension of our polychromatic source. Each spot has a vertical × horizontal FWHM size of 1.7 µm × 9.2 µm.

The *spectrometer stage* has the V-FM at 200 mm from the sample, delivering extreme vertical magnification of the image on the PSD to reduce the influence of its pixel size. The optical element dispersing the light in $h\nu_{out}$ is a spherical VLS grating with a central groove density a_0 = 3500 lines mm^{-1} installed at 1518 mm from the sample [optimization of the grating position and VLS parameters followed the procedure of Ghiringhelli *et al.* (2006)]. The VLS parameter a_2 was numerically optimized to cancel the asymmetric (coma) aberrations at a grating illumination of 100 mm, and a_3 to reduce the symmetric aberrations. The PSD, having an effective spatial resolution of 24 µm (typical of CCD detectors nowadays), is inclined at a grazing incidence angle of 20° in the horizontal plane to reduce the effective pixel size for $h\nu_{out}$. With the grating delivering a dispersion of ∼1.75 eV mm^{-1} along the PSD, its width of 20 mm allows parallel detection of an $h\nu_{out}$ range of 35 eV. Certainly the spectrometer stage can use alternative optical schemes such as that of Hettrick–Underwood (Hague *et al.*, 2005), bringing larger acceptance in the dispersive plane.

The image formed on the PSD is shown in Fig. 2(*c*). The monochromatic lines are now dispersed in $h\nu_{out}$ (= $h\nu_{in}$ in our case) in the horizontal direction. This image is therefore the full map of scattered intensity resolved in $h\nu_{in}$ and $h\nu_{out}$. In convolution with the PSD spatial resolution, the image demonstrates $E/\Delta E$ for $h\nu_{in}$ and $h\nu_{out}$ better than 11100 and

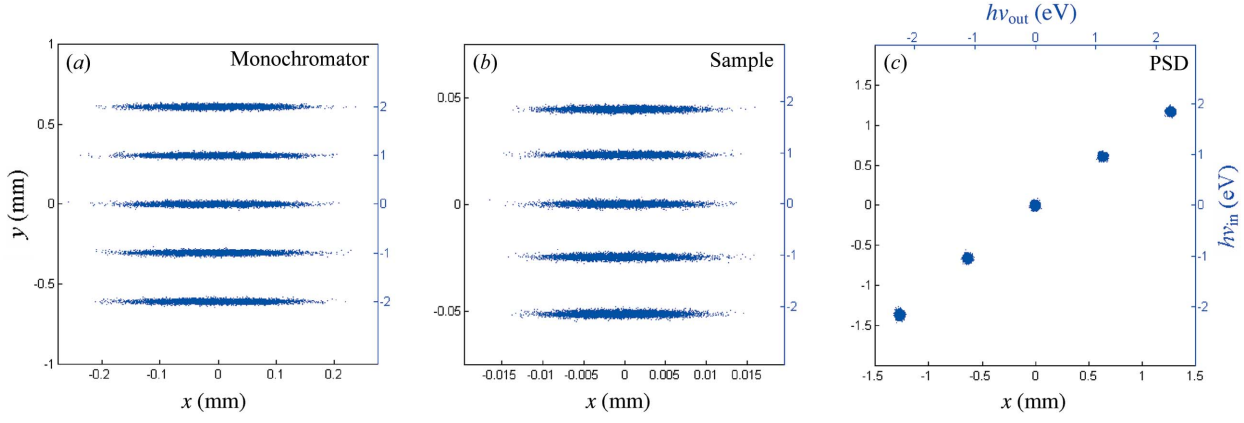

Figure 2
Ray-tracing simulations of images formed by five monochromatic rays separated by 1 eV (*a*) in the monochromator focal plane, (*b*) on the sample in scattered intensity seen by the spectrometer and (*c*) on the two-dimensional PSD resolved in $h\nu_{in}$ and $h\nu_{out}$. Note the different coordinate scales and the same $h\nu_{in}$ energy scale.

13700, respectively, allowing state-of-the-art RIXS experiments. Certain distortions of the $h\nu_{\rm in}$ scale can easily be corrected by post-processing of the data.

The above preliminary optical scheme has vast room for improvement. The resolution in $h\nu_{\rm in}$ can be increased by optimization of the refocusing stage vertical demagnification, which defines the vertical image size on the sample and thus on the PSD. Most importantly, one can implement the monochromator without any horizontal focusing to deliver divergent light directly to the H-RM. The concomitant increase in the horizontal demagnification by a factor of $\sim$3 will dramatically reduce the horizontal spot size on the sample and thus improve the spectrometer resolution in $h\nu_{\rm out}$. The XFEL sources with their low emittance and round spot profile allow further reduction of the horizontal spot size, with more relaxed demagnification and smaller footprint on the H-RM.

4. Summary

The concept of a spectrometer for resonant inelastic X-ray scattering – nicknamed $h\nu^2$ – has been presented where imaging and dispersion actions in the vertical and horizontal planes, respectively, are combined to deliver a full two-dimensional map of RIXS intensity in one shot with parallel detection in $h\nu_{\rm in}$ and $h\nu_{\rm out}$. Compared with the conventional RIXS spectrometers, this scheme is free of any compromise on energy resolution (with sufficient horizontal refocusing) or detection efficiency. Preliminary ray-tracing simulations with a typical third-generation synchrotron source demonstrate a resolving power above 11000 in $h\nu_{\rm in}$ and above 13700 in $h\nu_{\rm out}$ at 930 eV photon energy, with vast room for further improvements such as a monochromator without intermediate horizontal focusing. XFEL sources, characterized by low emittance and round spot profiles, simplify the refocusing stage and allow further increase of resolution. Owing to the one-shot operation principle of the $h\nu^2$ spectrometer, its combination with XFELs promises efficient time-resolved RIXS experiments.

The author thanks U. Flechsig for expert advice, and J. F. van der Veen, C. Quitmann, B. Patterson, R. Abela, Th. Schmitt and L. Patthey for encouragement and promoting discussions.

References

Agåker, M., Anderssson, J., Englund, C.-J., Olsson, A. & Nordgren, J. (2009). *Nucl. Instrum. Methods Phys. Res. A*, **601**, 213–219.
Bahrdt, J., Flechsig, U. & Senf, F. (1995). *Rev. Sci. Instrum.* **66**, 2719.
Bernstein, D. P., Acremann, Y., Scherz, A., Burkhardt, M., Stöhr, J., Beye, M., Schlotter, W. F., Beeck, T., Sorgenfrei, F., Pietzsch, A., Wurth, W. & Föhlisch, A. (2009). *Appl. Phys. Lett.* **95**, 134102.
Follath, R. & Senf, F. (1997). *Nucl. Instrum. Methods Phys. Res. A*, **390**, 388–394.
Fung, H. S., Chen, C. T., Huang, L. J., Chang, C. H., Chung, S. C., Wang, D. J., Tseng, T. C. & Tsang, K. L. (2004). *AIP Conf. Proc.* **705**, 655–658.
Ghiringhelli, G., Piazzalunga, A., Dallera, C., Trezzi, G., Braicovich, L., Schmitt, T., Strocov, V. N., Betemps, R., Patthey, L., Wang, X. & Grioni, M. (2006). *Rev. Sci. Instrum.* **77**, 113108.
Hague, C. F., Underwood, J. H., Avila, A., Delaunay, R., Ringuenet, H., Marsi, M. & Sacchi, M. (2005). *Rev. Sci. Instrum.* **76**, 023110.
Hatsui, T., Setoyama, H., Shigemasa, E. & Kosugi, N. (2005). *J. Electron Spectrosc. Relat. Phenom.* **144**, 1059.
Kotani, A. & Shin, S. (2001). *Rev. Mod. Phys.* **73**, 203–246.
Nordgren, J., Bray, J., Gramm, S., Nyholm, R., Rubensson, J.-E. & Wassdahl, N. (1989). *Rev. Sci. Instrum.* **60**, 1690.
Pascarelli, S., Mathon, O., Muñoz, M., Mairs, T. & Susini, J. (2006). *J. Synchrotron Rad.* **13**, 351–358.
Patterson, B. *et al.* (2009). In *Ultrafast Phenomena at the Nanoscale*, PSI Bereicht No. 09/10 (September 2009). PSI, Villigen, Switzerland.
Peatman, W. B. (1997). *Gratings, Mirrors and Slits – Beamline Design for Soft X-ray Synchrotron Radiation Sources.* Amsterdam: Gordon and Breach.
Schlappa, J. *et al.* (2009). *Phys. Rev. Lett.* **103**, 047401.
Strocov, V. N., Schmitt, T., Flechsig, U., Schmidt, T., Imhof, A., Chen, Q., Raabe, J., Betemps, R., Zimoch, D., Krempasky, J., Wang, X., Grioni, M., Piazzalunga, A. & Patthey, L. (2010). *J. Synchrotron Rad.* Submitted.
Strocov, V. N., Schmitt, T. & Patthey, L. (2008). PSI Technical Report SLS-SPC-TA-2008–309. PSI, Villigen, Switzerland. [Available at http://slsbd.psi.ch/pub/slsnotes/spcta080309.pdf.]
Tokushima, T., Harada, Y., Ohashi, H., Senba, Y. & Shin, S. (2006). *Rev. Sci. Instrum.* **77**, 063107.